

Optical method for measuring the azimuthal anchoring strength of liquid crystals using pitch values determined in imperfect samples

Tsung-Ta Tang, Hsin-Ying Wu, Chia-Jen Lin, and Ru-Pin Pan

Citation: [Journal of Applied Physics](#) **102**, 063108 (2007); doi: 10.1063/1.2781320

View online: <http://dx.doi.org/10.1063/1.2781320>

View Table of Contents: <http://scitation.aip.org/content/aip/journal/jap/102/6?ver=pdfcov>

Published by the [AIP Publishing](#)

Articles you may be interested in

[Optically activated shutter using a photo-tunable short-pitch chiral nematic liquid crystal](#)

Appl. Phys. Lett. **103**, 101105 (2013); 10.1063/1.4818679

[Fast-switching phase gratings using in-plane addressed short-pitch polymer stabilized chiral nematic liquid crystals](#)

Appl. Phys. Lett. **99**, 253502 (2011); 10.1063/1.3670041

[Spatially resolved lasers using a glassy cholesteric liquid crystal film with lateral pitch gradient](#)

Appl. Phys. Lett. **98**, 111112 (2011); 10.1063/1.3568889

[Simple method for measuring the azimuthal anchoring strength of nematic liquid crystals](#)

Appl. Phys. Lett. **79**, 2910 (2001); 10.1063/1.1415344

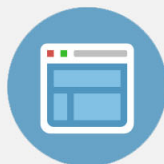
[Surface anchoring energy modulation in liquid crystal cells with mixed conductor boundary layers](#)

Appl. Phys. Lett. **78**, 2455 (2001); 10.1063/1.1368182



Re-register for Table of Content Alerts

Create a profile.



Sign up today!



Optical method for measuring the azimuthal anchoring strength of liquid crystals using pitch values determined in imperfect samples

Tsung-Ta Tang

Department of Photonics and Institute of Electro-Optical Engineering, National Chiao Tung University, 1001 Ta Hsueh Rd., Hsinchu, Taiwan, 30010, Republic of China

Hsin-Ying Wu, Chia-Jen Lin, and Ru-Pin Pan^{a)}

Department of Electrophysics, National Chiao Tung University, 1001 Ta Hsueh Rd., Hsinchu, Taiwan, 30010, Republic of China

(Received 23 April 2007; accepted 26 July 2007; published online 20 September 2007)

An improved Grandjean–Cano wedge method for measuring the pitch of a chiral nematic liquid crystal is demonstrated. This method is easy to implement and can yield results of high accuracy when it is used for measuring the liquid crystal surface anchoring strength. © 2007 American Institute of Physics. [DOI: [10.1063/1.2781320](https://doi.org/10.1063/1.2781320)]

I. INTRODUCTION

The anchoring strength at the liquid crystal (LC)–substrate interface is an important index of the alignment property in the development of new alignment methods, such as groove interface,^{1–3} SiO substrate,^{4,5} photoalignment,^{6,7} ion beam alignment,^{8,9} and other methods. Anchoring strength comprises polar anchoring strength that defines the surface energy of LC molecules and is related to the orientation out of the substrate plane, and azimuthal anchoring strength that describes the in-plane surface energy. Various methods for measuring azimuthal anchoring strength have been demonstrated. Most involve optical measurement of the polarization state by measuring the transmission of light through the LC cell and polarizers.^{10–13} In all of these methods, a known torque, induced by the application of an external field,^{14,15} the mixing of LC with chiral dopant,¹⁶ or the gliding of one substrate, is applied to the LC and the resulting rotation of the LC director (which is the unit vector describing the molecular orientation) at the surface is measured.

Test LC cells with antiparallel surface alignment and filled with a chiral doped nematic LC (NLC) are often used to measure azimuthal anchoring strength.¹⁶ By applying the elastic theory of LC, the azimuthal anchoring strength A can be expressed as

$$A = \frac{2K_{22}}{\sin \theta} \left(\frac{2\pi}{P} - \frac{\theta}{d} \right), \quad (1)$$

where K_{22} is the twist elastic constant, θ is the twist angle of chiral NLC in the cell, P is the natural pitch of the filled chiral NLC, and d is the thickness of the LC layer, or the cell gap.¹⁶ In this method, the values of P and θ are important. Their uncertainty affects the accuracy of azimuthal anchoring strength A .

The conventional method to determine the pitch is the Grandjean–Cano wedge method,¹⁷ which employs a wedge-shaped cell filled with the chiral NLC. Domains with twist

angles that are multiples of π are formed. The disclination lines are formed between two neighboring domains and can be seen both by the naked eye and under a microscope. The difference between the thicknesses of the LC layer at the adjacent disclination lines is half of the pitch. With a known wedge angle, the pitch can be determined by measuring the spacing between the adjacent disclination lines. However, the wedge is not perfect in reality, as the angles and the spacing between disclination lines are not uniform, because of bending or stress in the glass substrate. An uncertainty as large as 10% is common.

This work demonstrates an improved simple method for measuring the pitch, regardless of any imperfection of the wedge. When a typical sample is placed between a pair of polarizers, many bright and dark fringes are observed because of the birefringence of LC. The pitch value is determined by counting the number of fringes directly. Furthermore, we will show that the accuracy of the azimuthal anchoring strength determination can be increased by applying the pitch value that is determined this way, because the principle for determining the twist angle θ is the same as that, which underlies the method used herein to determine the pitch.

In Sec. II, we describe the experimental setup and theory for measuring pitch. In Sec. III, we show the improvement in the measurement of the azimuthal anchoring strength by applying the pitch that was determined by the presented method. Brief conclusions are given in the last section.

II. METHOD FOR PITCH MEASUREMENT

The wedged LC cell that we use to determine the pitch of chiral NLC has the same structure as that used in the Grandjean–Cano method. The cell is constructed with two glass substrates wedged with a piece of Mylar spacer at one end. The surfaces of the substrates are coated with polyimide SE-130B (from Nissan Co.) and rubbed with nylon fabric. The rubbing directions of the two substrates are antiparallel to each other. The cell is filled with NLC E7 (from Merck Co.), which is doped with chiral material ZLI-811 (from Merck Co.). A pair of crossed polarizers is used and the cell

^{a)}Electronic mail: rpchao@mail.nctu.edu.tw

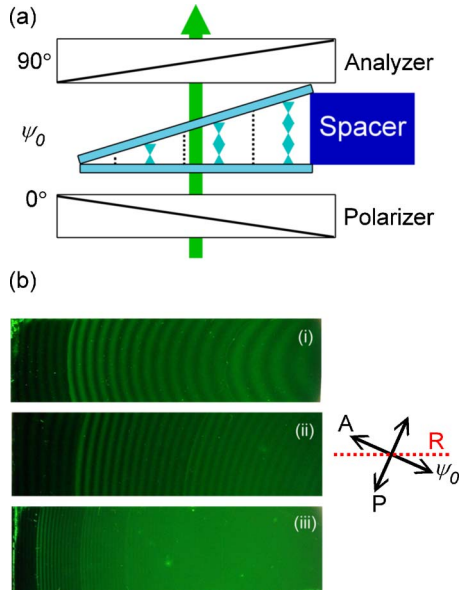


FIG. 1. (Color online) (a) Setup of the presented method. The incident light is monochromatic. (b) Photographs of wedged samples with different spacer thicknesses: (i) 50, (ii) 75, and (iii) 250 μm . A: analyzer, P: polarizer, and R: rubbing direction.

is placed between them, with the rubbing direction set at an angle ψ_0 from the polarizer transmission axis. An extended white light source, such as the common film viewer and a narrow color filter ($\lambda=546\text{ nm}$), was used and the sample yielded many bright and dark fringes between two adjacent disclination lines. Both the fringes and the disclination lines can be observed with the naked eye. In Fig. 1(a), we show the measuring system. Photographs of three samples with different wedge angles, using spacers of different thicknesses, are shown in Fig. 1(b).

By using the Jones matrix method, the optical transmittance T of a twist nematic liquid crystal cell between cross polarizers can be written as

$$T = \frac{1}{\Gamma^2 + 4\theta^2} \left\{ \left[\sqrt{\Gamma^2 + 4\theta^2} \cos\left(\frac{\sqrt{\Gamma^2 + 4\theta^2}}{2}\right) \sin(\theta) - 2\theta \cos(\theta) \sin\left(\frac{\sqrt{\Gamma^2 + 4\theta^2}}{2}\right) \right]^2 + \Gamma^2 \sin^2\left(\frac{\sqrt{\Gamma^2 + 4\theta^2}}{2}\right) \sin^2(\theta - 2\psi_0) \right\}, \quad (2)$$

where Δn is the birefringence of chiral NLC, λ is the wavelength of light, and d is the thickness of the LC layer. The phase retardation of the cell given by

$$\Gamma = 2\pi d \Delta n / \lambda. \quad (3)$$

Grandjean observed that a wedged chiral NLC cell prepared under planar alignment conditions generates disclination lines whenever the twist angle changes by π .¹⁸ In the region between the N th and the $(N+1)$ th disclination lines, the twist angle θ is fixed at $N\pi$, where $N=0, 1, 2$, etc., but the cell gap d in the wedge changes from $(2N-1)P/4$ to $(2N+1)P/4$ monotonically with position. Accordingly, the phase retardation, Γ , changes with position. The fringe pat-

terns that result in each domain are in accordance with Eq. (2). For $\lambda=546\text{ nm}$, $\Delta n=0.243$, and $P=56\text{ }\mu\text{m}$, the ratio θ/Γ is about 0.04, such that the twist angle is much smaller than the phase retardation. For $\theta/\Gamma \ll 1$, we can rewrite Eq. (2) in terms of θ/Γ and $(\theta/\Gamma)^2$ and omit the higher order terms as follows:

$$T = \frac{1}{2} \left[\sin^2(2\psi_0) + 4\frac{\theta^2}{\Gamma^2} \right] \left\{ 1 - \cos \left[\Gamma \left(1 + 2\frac{\theta^2}{\Gamma^2} \right) \right] \right\}. \quad (4)$$

The right-hand side of the equation is a product of two factors and the constant $1/2$. The first factor represents the transmittance amplitude, which increases with the twist angle θ of each domain. For $\psi_0=45^\circ$, this factor is close to 1 for each domain; therefore, the peak intensities in all domains are almost the same. However, when ψ_0 is small, an abrupt change in this amplitude occurs at the disclination lines, where the twist angle changes by π abruptly as shown in Fig. 1(b). The distinct change of transmittance offers another means of distinguishing the disclination lines. The second factor in Eq. (4) describes the fringe behavior within each domain. Since $2\theta^2/\Gamma^2$ is much smaller than one, the fringe intensity is approximately a sinusoidal function of phase retardation Γ .

The change in Γ between any two fringe lines (dark lines or bright lines) is 2π , which corresponds to a change of $\lambda/\Delta n$ in cell gap d , as given by Eq. (3). With a total of N_f fringe lines in each domain, the change in total thickness is $N_f \lambda / \Delta n$. However, the difference between the cell gaps at two adjacent disclination lines is $P/2$. Therefore, the pitch P can be determined by simply counting the fringe number N_f in each domain and then applying the simple relation

$$P = 2N_f \lambda / \Delta n. \quad (5)$$

In this method we do not need to know the wedge angle, which is required in the traditional Grandjean–Cano method. Instead, the value of Δn is important in obtaining an accurate pitch value. In the next section, however, we will show that even the error that is caused by Δn will be cancelled out for measuring anchoring strength.

III. EFFECT ON AZIMUTHAL ANCHORING STRENGTH

As mentioned earlier, this work presents a simple method for measuring the pitch of chiral NLC, which is used in an antiparallel cell to measure azimuthal anchoring strength. As described in Sec. I and by Eq. (1), the determination of the twist angle θ is the main part of the measurement of the azimuthal anchoring strength. This angle can be measured using an optical method that is based on the transmittance relation

$$T = \left[\frac{1}{\sqrt{1+u^2}} \sin(\sqrt{1+u^2}\theta) \sin(\theta - \psi_{pol}) + \cos(\sqrt{1+u^2}\theta) \cos(\theta - \psi_{pol}) \right]^2 + \frac{u^2}{1+u^2} \sin^2(\sqrt{1+u^2}\theta) \cos^2(\theta + 2\psi_0 - \psi_{pol}), \quad (6)$$

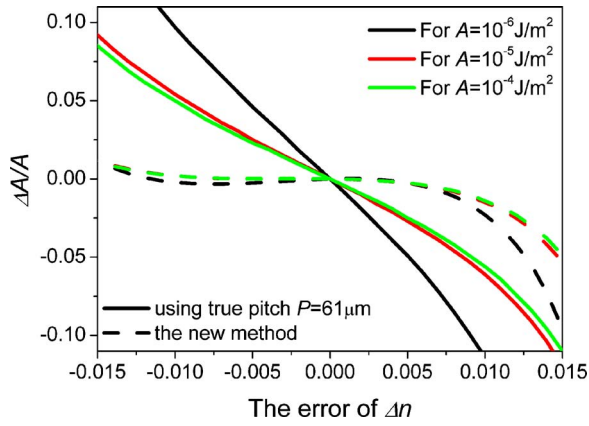


FIG. 2. (Color online) Analysis of error of anchoring strength, $\Delta A/A$, vs error in birefringence Δn . Solid curves are calculated using the true pitch value. Dashed curves are calculated using the pitch value measured with the presented method.

where ψ_{pol} is the angle between the transmission axes of the analyzer and the polarizer, $u = \pi d \Delta n / (\lambda \theta)$. Varying the angles of the sample and polarizer and determining the minimum transmittance enable the twist angle θ to be determined. Both Eqs. (2) and (6) are based on the same principle, only that here the thickness is a constant and the angle ψ_{pol} is allowed to vary. Knowledge of Δn is also required to determine the twist angle.

Since birefringence Δn is used in determining both the value P and the twist angle θ to obtain the azimuthal anchoring strength according to Eq. (1), the error in the azimuthal anchoring strength caused by any error in birefringence Δn is now considered. If the same error of Δn is introduced in measuring both the pitch and the twist angle, then what is the resulting error ΔA in the final measurement of the anchoring strength? Consider a hypothetical cell with a LC thickness of $11.5 \mu\text{m}$, a true pitch P of $6.1 \mu\text{m}$, a twist elastic constant K_{22} of $6.1 \times 10^{-12} \text{ N}$, and a Δn of 0.223. Suppose that the surface has a true anchoring strength A whose value lies anywhere between 10^{-3} and 10^{-6} J/m^2 . With this A value, the cell has a definite twist angle θ , according to Eq. (1). Hence, the angle ψ_{pol} that minimizes the intensity can be determined from Eq. (6). Experimentally, the angle ψ_{pol} is measured to deduce θ . However, if an error Δn_{error} applies to Δn , then the deduced value θ' and the pitch value P' that is determined by the presented method differ from the true θ and P , respectively. Then, the anchoring strength A' that was calculated using Eq. (1) differs from the true value of A , but with an error of ΔA or $A' - A$. Figure 2 shows the calculated $\Delta A/A$ against Δn_{error} for four values of A with a wavelength of $0.6328 \mu\text{m}$. The anchoring strengths A' of the solid curves are calculated using Eq. (1) with the deduced twist angle θ' and the true pitch P . The error in A can exceed 5% if Δn_{error} is 0.01 (or 4%). The pitch value P' measured by the presented method was substituted into Eq. (1) to yield the calculated error $\Delta A/A$ that is also plotted in Fig. 2 with dashed curves. The error is negligible for $\Delta n_{\text{error}} \leq 0.01$. For $A > 10^{-3} \text{ J/m}^2$, the curves of $\Delta A/A$ almost overlap that for $A = 10^{-4} \text{ J/m}^2$. At $\Delta n_{\text{error}} \approx \pm 0.015$, the values of $d\Delta n/\lambda$ are close to half integers. This is a condition of singularity in the measurement, which should be avoided.¹⁹

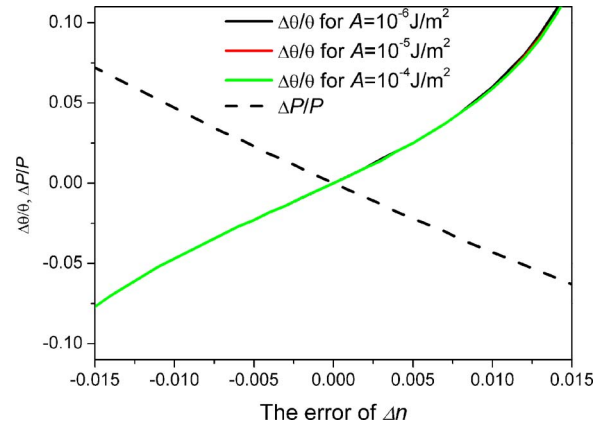


FIG. 3. (Color online) Solid curves plot the error ratio $\Delta\theta/\theta$ vs A . Dashed lines plot $\Delta P/P$ vs A .

Now, the cause of the drastic reduction in error is analytically examined using the measured P' value to deduce the anchoring strength. By differentiating Eq. (1), we obtain

$$\Delta A = \left(-A \theta \cot \theta - \frac{2K_{22} \theta}{\sin \theta d} \right) \frac{\Delta \theta}{\theta} + \left(-\frac{4\pi K_{22}}{P \sin \theta} \right) \frac{\Delta P}{P}. \quad (7)$$

Dividing Eq. (7) by A in Eq. (1) yields

$$\frac{\Delta A}{A} = \left[(-\theta \cot \theta) - \frac{\frac{\theta}{d}}{\left(\frac{2\pi}{P} - \frac{\theta}{d} \right)} \right] \frac{\Delta \theta}{\theta} + \left[-1 - \frac{\frac{\theta}{d}}{\left(\frac{2\pi}{P} - \frac{\theta}{d} \right)} \right] \frac{\Delta P}{P}. \quad (8)$$

The two errors $\Delta\theta/\theta$ and $\Delta P/P$ were caused by Δn_{error} using Eqs. (1), (5), and (6). The results are plotted in Fig. 3. The solid curves are $\Delta\theta/\theta$ for several A values and the dashed curve is for $\Delta P/P$. The $\Delta\theta/\theta$ values depend only weakly on A . Figure 3 shows that approximately

$$\frac{\Delta P}{P} = -\frac{\Delta \theta}{\theta}. \quad (9)$$

Substituting the approximation Eq. (9) into Eq. (8) cancels out most parts of Eq. (8). Equation (8) can be rewritten as

$$\frac{\Delta A}{A} = (1 - \theta \cot \theta) \frac{\Delta \theta}{\theta}. \quad (10)$$

The relationships among θ , $\theta \cot \theta$, and the anchoring strength are plotted in Fig. 4(a). When the anchoring strength exceeds 10^{-5} J/m^2 , the product of θ and $\cot \theta$ is almost equal to one and $\Delta A/A$ in Eq. (10) is roughly equal to zero.

However, if the true pitch is used in determining the anchoring strength, ΔP is zero and the second term of Eq. (8) does not exist. In this case,

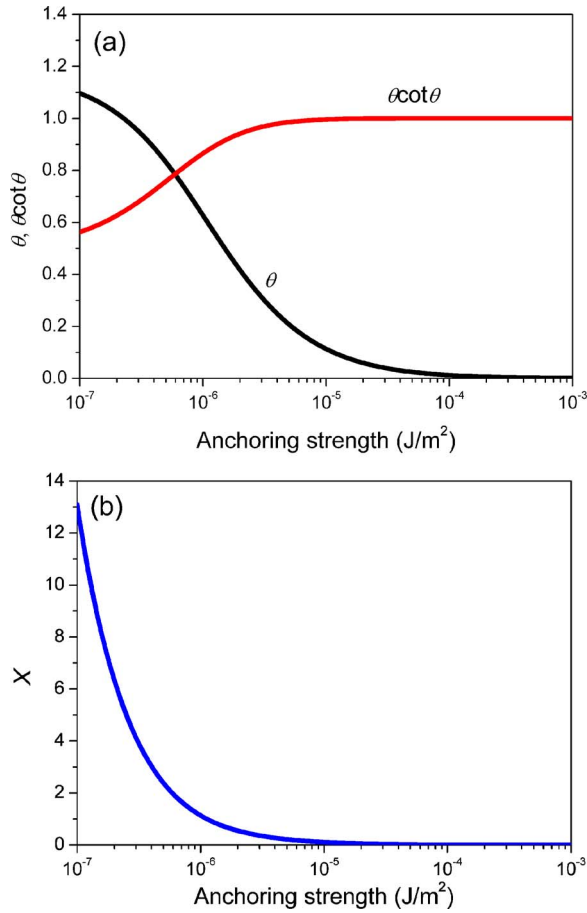


FIG. 4. (Color online) (a) Relationships among twist angle θ , $\theta \cot \theta$, and anchoring strength and (b) relationship between $X = (\theta/d)/(2\pi/P - \theta/d)$ and anchoring strength.

$$\frac{\Delta A}{A} = \left(-\theta \cot \theta - \frac{\frac{\theta}{d}}{\frac{2\pi}{P} - \frac{\theta}{d}} \right) \frac{\Delta \theta}{\theta}. \quad (11)$$

Figure 4(b) plots relationship between the second term in parentheses, $X = (\theta/d)/(2\pi/P - \theta/d)$, and the anchoring strength A . This value is almost zero when $A > 10^{-5} \text{ J/m}^2$. Then $|\Delta A/A|$ becomes $|\Delta \theta/\theta|$. For $A \leq 10^{-6} \text{ J/m}^2$, the X value significantly exceeds $\theta \cot \theta$. Hence, $|\Delta A/A|$ is roughly equal to $X|\Delta \theta/\theta|$, which exceeds $|\Delta \theta/\theta|$. In any case, the error here is much larger than that calculated using the measured pitch value. When the anchoring strength is smaller, this effect is more prominent.

IV. CONCLUSION

This work developed a simple method for measuring pitch value. The sensitivity of the method is $\pm \lambda/2\Delta n$. This method is useful for pitch values that exceed several tens of micrometers, which values for pitch are commonly used to measure azimuthal anchoring strength. This method does not require the knowledge of the wedge angle of the cells but rather requires the birefringence value of NLC. This fact seems to be a shortcoming of this method; however, this measured pitch value can be used to deduce a more accurate anchoring strength than that can be obtained the true pitch value. According to the simulation based on the calculations herein, the error in the anchoring strength determination can be reduced by a factor of about 10.

ACKNOWLEDGMENTS

This work was supported by the National Science Council of the Republic of China under Grant No. NSC95-2221-E-009-249, MOE ATU Program, and PPAEU-II.

- ¹D. W. Berreman, Phys. Rev. Lett. **28**, 1683 (1972).
- ²S. Faetti, Phys. Rev. A **36**, 408 (1987).
- ³Y. F. Lin, S. Y. Lu, and R. P. Pan, Jpn. J. Appl. Phys. **44**, 8552 (2005).
- ⁴S. Faetti, M. Gatti, V. Palleschi, and T. J. Sluckin, Phys. Rev. Lett. **55**, 1681 (1985).
- ⁵H. Yokoyama, S. Kobayashi, and H. Kamei, J. Appl. Phys. **61**, 4501 (1987).
- ⁶B. R. Acharya, J. H. Kim, and S. Kumar, Jpn. J. Appl. Phys., Part 2 **38**, L1538 (1999).
- ⁷M. Hasegawa, Jpn. J. Appl. Phys., Part 2 **41**, L1167 (2002).
- ⁸J. P. Doyle, P. Chaudhari, J. L. Lacey, E. A. Galligan, S. C. Lien, A. C. Callegari, N. D. Lang, M. Lu, Y. Nakagawa, H. Nakano, N. Okazaki, S. Odahara, Y. Katoh, Y. Saitoh, K. Sakai, H. Satoh, and Y. Shiota, Nucl. Instrum. Methods Phys. Res. B **206**, 467 (2003).
- ⁹S. J. Chang, K. Y. Wu, Y. H. Yang, J. Hwang, H. Y. Wu, R. P. Pan, A. P. Lee, and C. S. Kou, Thin Solid Films **515**, 8000 (2007).
- ¹⁰Y. Iimura, N. Kobayashi, and S. Kobayashi, Jpn. J. Appl. Phys., Part 2 **33**, L434 (1994).
- ¹¹T. Akahane, H. Kaneko, and M. Kimura, Jpn. J. Appl. Phys., Part 1 **35**, 4434 (1996).
- ¹²J. G. Fonseca and Y. Galerne, Appl. Phys. Lett. **79**, 2910 (2001).
- ¹³M. Kawamura, Y. Goto, and S. Sato, Jpn. J. Appl. Phys., Part 1 **43**, 6239 (2004).
- ¹⁴T. Oh-ide, S. Kuniyasu, and S. Kobayashi, Mol. Cryst. Liq. Cryst. **164**, 91 (1988).
- ¹⁵S. Faetti and G. C. Mutinati, Phys. Rev. E **68**, 026601 (2003).
- ¹⁶Y. Sato, K. Sato, and T. Uchida, Jpn. J. Appl. Phys., Part 2 **31**, L579 (1992).
- ¹⁷R. Cano, Bull. Soc. Fr. Mineral. Cristallogr. **91**, 20 (1968).
- ¹⁸M. F. Grandjean, C. R. Hebd. Seances Acad. Sci. **71**, 172 (1921).
- ¹⁹Y. Saitoh and A. Lien, Jpn. J. Appl. Phys., Part 1 **39**, 1743 (2000).